ENGINEERING RESEARCH INSTITUTE
THE UNIVERSITY OF MICHIGAN
ANN ARBOR

Final Report

A PRELIMINARY REPORT ON THE DETERMINATION OF STRESSES IN THIN PROPELLER BLADES

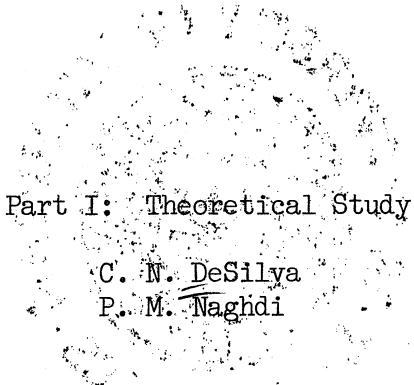

Part I: Theoretical Study

C. N. DeSilva
P. M. Naghdi

Part II: Experimental Study

S. K. Clark

Project 2528

WRIGHT AIR DEVELOPMENT CENTER
WRIGHT-PATTERSON AIR FORCE BASE, OHIO
CONTRACT NO AF 33(616)-3590

September 1957

TABLE OF CONTENTS

PART I

THEORETICAL STUDY

by

C. N. DeSilva and P. M. Naghdi

ACKNOWLEDGEMENT

The authors gratefully acknowledge the assistance of Mrs. B. T. Caldwell in the various parts of this report. The Appendix pertaining to the load on the propeller blade was prepared entirely by her.

PREFACE

In order to absorb the enormous power of modern aircraft engines, the propeller blade must be so designed that its airfoil section merges into the round shank at the spinner within a very short length. This region from the airfoil to the shank - the so-called transition region - becomes highly stressed during operational conditions. The bounding surface of this region is not simple; indeed, its mathematical specification becomes very difficult. The ordinary simple methods of stress analysis fail to predict even approximately the stresses developed in such a propeller blade. Thus, it becomes necessary to employ more stringent and accurate theories to determine the stress distribution. In the present report, we confine ourselves to the "hollow blade" design of such a propeller and apply the bending theory of shells in an attempt to find the stresses within the propeller. This is no easy task especially for the transition region, where, as was mentioned, the bounding surface is mathematically difficult to prescribe. The present report summarizes only the theoretical work accomplished so far, work which is substantial indeed but still requires considerable effort to bring to completion. Hence, this report must be regarded as containing only the preliminary work on the project.

1. INTRODUCTION

In order to apply the theory of thin elastic shells to find the stress distribution in the hollow blade propeller, we have shown in Fig. 1 a simplified middle surface of the blade. It is evident by inspection that this middle surface can be subdivided into three component parts as follows: Part A is the airfoil region. The transverse section of Part A (transverse implying perpendicular to the axis of the blade) is an ellipse. The airfoil region will therefore be treated as an elliptic cylindrical shell. Part B is the transition region. This is the region in which the elliptic cylinder of Part A changes into Part C which is the round shank. The transverse section of Part C is a circle, allowing this region to be treated as a circular cylindrical shell.

Before proceeding to a detailed examination of these component parts of the propeller, a word about the loading is in order. From physical tests, it has been found that the lift coefficient may be assumed, with negligible error, to exist only on the airfoil region. Thus, Parts B and C may be assumed free of surface loads while a variable surface load acts on Part A. All three blad regions, however, will be subjected to a centrifugal force due to rotation of the blade. For the sake of generality, however, no assumption will be made here about the character of the loading.

2. PART A: THE AIRFOIL SECTION

A. THE GEOMETRY OF THE SECTION

The airfoil section is of constant thickness $h = h_A$ and will be treated as a thin elliptical cylindrical shell. The transverse section is an ellipse η_o represented by

$$x = a_1 \sin \phi \tag{2.1}$$

$$y = b_1 \cos \phi \tag{2.2}$$

where a_1 and b_1 are the lengths of the semi-major and semi-minor axes of the ellipse, respectively. The angle $\phi = \phi_A$, as well as x_A, the arc length of η_o, are measured clockwise from the vertical axis.

Let $\vec{a}_3$ be the unit normal vector to the middle surface $\overline{M}$ of the shell and let ζ be the distance along $\vec{a}_3$ of a point from $\overline{M}$, such that $\zeta = \pm h_A/2$ defines the two surfaces which are the boundaries of a shell of thickness h_A. Then the position vector of a point of the shell is $\vec{R} = L_A \vec{R}_1 + \zeta \vec{a}_3$,

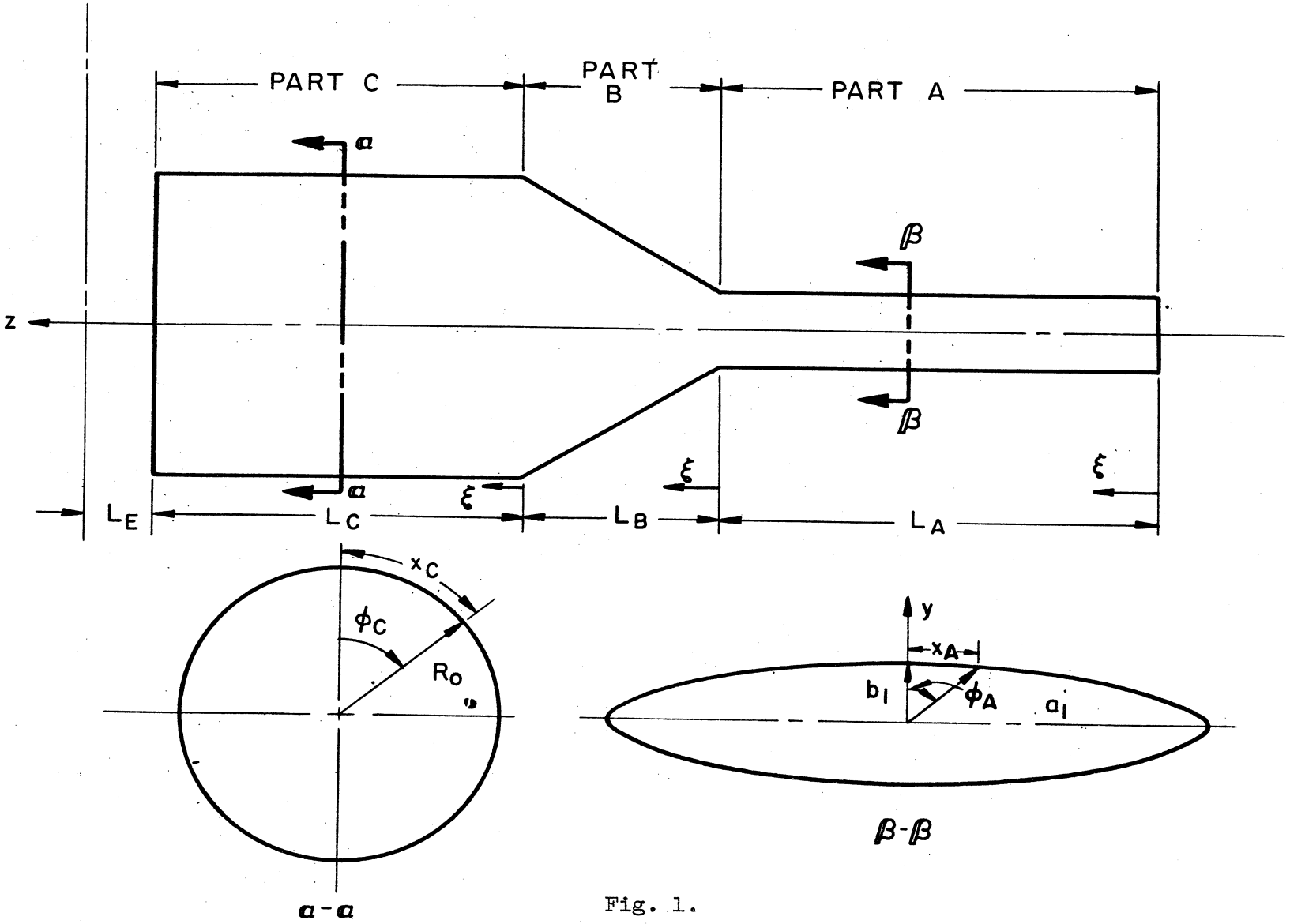
PART C
PART B
PART A
α
β
z
ξ
L_E
L_C
L_B
L_A
x_C
ϕ_C
R_o
α-α
y
x_A
b_1
ϕ_A
a_1
β-β

Fig. 1.

where L_A is a characteristic length and $L_A \vec{R}_1$ denotes the position vector of a point on $\overline{M}$. The equation of the line element of the shell is given by

$$ds^2 = g_{11}\, d\phi^2 + dz^2 + d\zeta^2 \tag{2.3}$$

where

$$g_{11} = a_1^2\, \beta_1^2\, (1 + k_1^2 \cos^2 \phi)$$

$$\beta_1 = \frac{b_1}{a_1} \tag{2.4}$$

$$k_1^2 = (1 - \beta_1^2)/\beta_1^2$$

and

$$x_A = a_1\, \beta_1 \int_0^{\phi} (1 + k_1^2 \cos^2 t)^{1/2}\, dt \tag{2.5}$$

which can easily be expressed in terms of elliptic integrals. We also note that R_A, the radius of curvature of the ellipse, is given by

$$R_A = a_1\, \beta_1^2\, (1 + k_1^2 \cos^2 \phi)^{3/2} \tag{2.6}$$

and that

$$R_{A_{min}} = R_A(\pi/2) = a_1\, \beta_1^2$$

$$0 \le \beta_1 \le 1 \tag{2.7}$$

$$R_{A_{max}} = R_A(0) = \frac{a_1}{\beta_1}$$

B. FORMULATION OF THE PROBLEM

Following the theory of cylindrical shells, as given in Ref. 1, the determination of the stress distribution is reduced to establishing a stress function Φ and a dimensionless displacement w normal to the middle surface. With the introduction of dimensionless coordinates

$$\theta = \frac{x_A}{s}, \quad \xi = \xi_A = \frac{z}{\ell_A}, \quad \eta = \frac{\zeta}{h_A} \tag{2.8}$$

we define

$$p_\theta = \frac{L_A}{\beta} P_\theta , \quad p_\xi = \frac{L_A}{\alpha} P_\xi , \quad p = L_A P$$

$$A_\theta = \int_{\theta_o}^{\theta} p_\theta \, dt , \quad A_\xi = \int_{\xi_o}^{\xi} p \, dt \tag{2.9}$$

In the above equations, P_θ, P_ξ, and P are the components of the load intensity in the θ, ξ, and η directions, respectively

$$\alpha = \frac{\ell_A}{L_A} , \qquad \beta = \frac{s}{L_A}$$

$$L_A = \min \begin{cases} \ell_A \\ s \\ R_{A_{min}} \end{cases} \tag{2.10}$$

ℓ_A is the span of the shell (see Fig. 1) and S is the circumference of the elliptic section η_o.

The differential equations for the deflection w and the function Φ may be written as (Ref. 1, p. 422)

$$LL(\psi) - i \epsilon^2 \psi_{,\xi\xi} = \Omega \tag{2.11}$$

where the comma denotes partial differentiation and

$$L( ) \equiv \alpha^2 ( )_{,\theta\theta} + \beta^2 ( )_{,\xi\xi} \tag{2.12}$$

$$\left.\begin{aligned} \psi &= w + i \bar{K} \bar{\Phi} \\ \Omega &= \bar{q} + i \bar{K} q \end{aligned}\right\} \tag{2.13}$$

$$\left.\begin{aligned} \epsilon^2 &= \frac{m \alpha^2 \beta^3 \rho}{\lambda} , \quad i = \sqrt{-1} \\ \bar{K} &= \left(\frac{\alpha\beta}{\lambda}\right)^2 \frac{m}{E L_A} , \quad m = \sqrt{12(1-\nu^2)} \\ \bar{q} &= \frac{\alpha^4 \beta^4}{B} (\beta \rho A_\theta + p) \end{aligned}\right\} \tag{2.14}$$

$$q = \alpha^4 A_{\xi,\theta\theta} + \beta^4 A_{\theta,\xi\xi} - \nu\alpha^2\beta^2 (p_{\xi,\xi} + p_{\theta,\theta})$$

$$\rho = \frac{s}{R_A} = \frac{s}{a_1\beta_1^2} (1 + k_1^2 \cos^2\phi)^{-3/2} \qquad (2.14)$$

Also the stress resultants and the stress couple may be expressed as

$$N_\theta = \beta^2 n_\theta , \quad N_\xi = \alpha^2 n_\xi , \quad N_{\theta\xi} = \alpha\beta n_{\theta\xi}$$

$$M_\theta = L_A \beta^2 m_\theta , \quad M_\xi = - L_A \alpha^2 m_\xi , \quad M_{\xi\theta} = - M_{\theta\xi} = \alpha\beta L_A m_{\theta\xi} \qquad (2.15)$$

$$Q_\theta = \beta q_\theta , \quad Q_\xi = \alpha q_\xi$$

where

$$m_\theta = - \frac{B}{\beta^2} \left[\frac{1}{\beta^2} w_{,\theta\theta} + \frac{\nu}{\alpha^2} w_{,\xi\xi} \right]$$

$$m_\xi = - \frac{B}{\alpha^2} \left[\frac{\nu}{\beta^2} w_{,\theta\theta} + \frac{1}{\alpha^2} w_{,\xi\xi} \right]$$

$$m_{\theta\xi} = - \frac{B(1-\nu)}{\alpha^2 \beta^2} w_{,\theta\xi} \qquad (2.16)$$

$$n_\theta = \Phi_{,\xi\xi} - A_\theta ; \quad n_\xi = \Phi_{,\theta\theta} - A_\xi ; \quad n_{\theta\xi} = - \Phi_{,\theta\xi}$$

$$q_\theta = m_{\theta,\theta} + m_{\theta\xi,\xi} , \quad q_\xi = m_{\theta\xi,\theta} + m_{\xi,\xi}$$

$$B = \frac{\lambda^3 E L_A}{12(1-\nu^2)} , \quad \lambda = \frac{h_A}{L_A} \qquad (2.17)$$

and E and ν are Young's modulus and Poisson's ratio, respectively.

C. SOLUTION OF THE HOMOGENEOUS DIFFERENTIAL EQUATION (2.11)

Assuming that ψ has the form

$$\psi = e^{i\gamma\xi}\, g(\theta) \tag{2.18}$$

where γ is some constant, then with the use of (2.12), the homogeneous equation (2.11) may be written as

$$\frac{d^4g}{d\theta^4} + C_1 \frac{d^2g}{d\theta^2} + [C_2 + C_3\, \epsilon^2(\theta)]g = 0 \tag{2.19}$$

In (2.19), C_j are constants defined as follows:

$$C_1 = -2\frac{\beta^2\gamma^2}{\alpha^2}, \qquad C_2 = \frac{\beta^4\gamma^4}{\alpha^4}, \qquad C_3 = i\frac{\gamma^2}{\alpha^4} \tag{2.20}$$

Since from (2.5) and (2.8), θ is a function of ϕ, being defined for $0 \leq \phi \leq 2\pi$, we now transform (2.19) so that ϕ becomes the independent variable. As a result of this transformation, (2.19) can be now written in the following form:

$$\frac{d^4g}{d\phi^4} + \mathcal{A}\frac{d^3g}{d\phi^3} + \mathcal{B}\frac{d^2g}{d\phi^2} + \mathcal{C}\frac{dg}{d\phi} + \mathcal{D}g = 0 \tag{2.21}$$

In (2.21), the following definitions hold:

$$\mathcal{A} = 3\, k_1^2 \sin 2\phi\, \Delta^{-1}$$

$$\mathcal{B} = k_1^2 [4(1+k_1^2) + \sin^2\phi\,(7\, k_1^2 - 8) - 11\, k_1^2 \sin^4\phi]\, \Delta^{-2}$$

$$- 2\frac{\beta^2\gamma^2}{\alpha^2}\left(\frac{\alpha_1\beta_1}{s}\right)^2 \Delta$$

$$\mathcal{C} = k_1^2 \cos\phi \sin\phi\, [-4 + 5\, k_1^2 + 9\, k_1^4 - 18\, k_1^2 \sin^2\phi - 3\, k_1^4 \sin^2\phi$$

$$- 6\, k_1^4 \sin^4\phi]\, \Delta^{-3} \tag{2.22}$$

$$- 2\left(\frac{\beta^2\gamma^2}{\alpha^2}\right) k_1^2 \cos\phi \sin\phi \left(\frac{a_1\beta_1}{s}\right)^2$$

$$\mathcal{D} = \frac{\beta^4\gamma^4}{\alpha^4}\left(\frac{a_1\beta_1}{s}\right)^4 \Delta^2 + i\frac{\gamma^2 m\beta^3}{\alpha^2\lambda\beta_1}\left(\frac{\alpha_1\beta_1}{s}\right)^3 \Delta^{1/2}$$

$$\Delta = (1 + k_1^2 \cos^2\phi)$$

Recalling from (2.4) that

$$k_1^2 = \frac{1 - \beta_1^2}{\beta_1^2}, \qquad \beta_1 = \frac{b_1}{a_1}$$

then under the restriction $0 \leq \beta_1 \leq 1$, we note that Δ is analytic and non-vanishing in I_ϕ: $0 \leq \phi \leq 2\pi$. It follows, therefore, that $\mathcal{A}$, $\mathcal{B}$, $\mathcal{C}$, and $\mathcal{D}$ are analytic in I_ϕ.

Since ϕ appears only as trigonometric functions in the coefficients of (2.21), we introduce a new variable χ as follows

$$\chi = \cos \phi$$

into the homogeneous equation (2.21) which becomes

$$(1 - \chi^2)^2 \, g^{iv} + [- 6\chi(1 - \chi^2) - (1 - \chi^2)^{3/2}\mathcal{A}] \, g'''$$

$$+ [- 4 + 7\chi^2 + 3\mathcal{A}\chi(1 - \chi^2)^{1/2} + \mathcal{B}(1 - \chi^2)] \, g''$$

$$+ [\chi + \mathcal{A}(1 - \chi^2)^{1/2} - \mathcal{B}\chi - \mathcal{C}(1 - \chi^2)^{1/2}] \, g'$$

$$+ \mathcal{D} g = 0$$

Here primes denote differentiation with respect to χ. After manipulation, this equation may be written in the form

$$(\chi - 1)^4 \, g^{iv} + a_1(\chi) \, (\chi - 1)^3 \, g''' + a_2(\chi) \, (\chi - 1)^2 \, g''$$

$$+ a_3(\chi) \, (\chi - 1) \, g' + a_4(\chi) \, g = 0 \qquad (2.23)$$

where

$$\left.\begin{aligned}
a_1(\chi) &= \frac{6 (1 + k_1^2) \chi}{(1 + k_1^2 \chi^2) (\chi + 1)} \\
a_2(\chi) &= \frac{2 \beta^2 \gamma^2}{\alpha^2} \left(\frac{a_1 \beta_1}{S}\right)^2 \frac{(1 + k_1^2 \chi^2) (\chi - 1)}{(\chi + 1)} \\
&\quad + \frac{(1 + k_1^2) [- 4 + (7 + 15 k_1^2) \chi^2 - 12 k_1^2 \chi^4]}{(1 + k_1^2 \chi^2)^2 (\chi + 1)^2} \\
a_3(\chi) &= \frac{2 \beta^2 \gamma^2}{\alpha^2} \left(\frac{a_1 \beta_1}{S}\right)^2 \frac{(1 + k_1^2) \chi (\chi - 1)}{(\chi + 1)^2} \\
&\quad + \frac{(1 + k_1^2) \chi (\chi - 1)}{(1 + k_1^2 \chi^2)^3 (\chi + 1)^2} [(1 + 13 k_1^2) - 15 k_1^2 (1 + k_1^2) \chi^2 + 12 k_1^4 \chi^4]
\end{aligned}\right\} \qquad (2.24)$$

$$a_4(\chi) = \frac{\beta^4\gamma^4}{\alpha^4}\left(\frac{a_1\beta_1}{s}\right)^4 \frac{(1 + k_1^2\chi^2)^2\,(\chi - 1)^2}{(\chi + 1)^2}$$

$$+ i\,\frac{\gamma^2 m\beta^3}{\alpha^2\lambda\beta_1}\left(\frac{a_1\beta_1}{s}\right)^3 \frac{(1 + k_1^2\chi^2)^{1/2}\,(\chi - 1)^2}{(\chi + 1)^2}$$

It will be noted that the a_j are analytic at $\chi = 1$ and have poles at $\chi = -1$. It follows then, from the form of (2.23), that $\chi = 1$ is a regular singular point of the differential equation and solutions may be found which are valid in the circular region with $\chi = 1$ as center and extending to the pole $\chi = -1$. Assume a solution of the form

$$g(\chi) = \sum_{n=0}^{\infty} c_n\,(\chi - 1)^{n+r_j} \tag{2.25}$$

where r_j are the solutions of the indicial equation

$$r(r-1)(r-2)(r-3) + a_1(1)\,r(r-1)(r-2)$$

$$+ a_2(1)\,r(r-1) + a_3(1)r + a_4(1) = 0$$

From (2.24), at $\chi = 1$, we have

$$a_1(1) = 3 \qquad a_3(1) = 0$$

$$a_2(1) = 3/4 \qquad a_4(1) = 0$$

Hence, the indicial equation reduces to the form

$$r(r-1)(r-1/2)(r-3/2) = 0$$

the roots of which are

$$r_j = \begin{cases} 0 \\ 1/2 \\ 1 \\ 3/2 \end{cases} \tag{2.26}$$

Solutions of the form (2.25) will exist for $r = 3/2$ and $r = 1$. The other two solutions will probably contain a term in $\log \chi$.

D. LOADING OF THE ELLIPTIC CYLINDER

The loading is described in detail in the Appendix.

3. PART C: THE ROUND SHANK

A. GEOMETRY AND FORMULATION OF THE PROBLEM

This component of the propeller blade will be treated at this time because it is a circular cylindrical shell, i.e., it is a special case of the elliptic cylindrical shell the theory of which was given in the previous sections. We have

$$a_1 = b_1 = R_o \; ; \qquad \beta_1 = 1 \tag{3.1}$$

It follows then that

$$\begin{aligned} s &= 2\pi R_o & \alpha &= \ell_c/L_c \\ \rho &= 2\pi & \beta &= 2\pi R_o/L_c \\ L_c &= \min\begin{cases} \ell_c \\ R_o \end{cases} & \lambda &= h_c/L_c \end{aligned} \tag{3.2}$$

where ℓ_c is the length of the round shank measured along the axis of the propeller (see Fig. 1).

The dimensionless coordinates θ, ξ, and η are now defined as

$$\theta = \frac{x_c}{s} \; , \qquad \xi = \frac{z - \ell_B - \ell_A}{\ell_c} \; , \qquad \eta = \frac{\zeta}{h_c}$$

$$x_c = R_o \phi_c \tag{3.3}$$

where the length x_c and the angle ϕ_c are both measured from the vertical axis, and h_c, which is a constant, is the thickness of the shell. All the previous expressions for the displacements and stresses still hold. The differential equation to be solved is again given by

$$LL(\psi) - i\,\epsilon^2\,\psi_{,\xi\xi} = \Omega \tag{3.4}$$

where the definitions of (2.12), (2.13), and (2.14) hold and it must be noted that ϵ^2 is a constant because of (3.2), viz.,

$$\epsilon^2 = 2m\,\alpha^2\beta^3\pi/\lambda \tag{3.5}$$

B. SOLUTION OF THE HOMOGENEOUS DIFFERENTIAL EQUATION (3.4)

Consider the homogeneous equation (3.4) which, by virtue of the definition of $L(\psi)$, may be written as

$$\frac{\partial^4\psi}{\partial\theta^4} + 2\frac{\beta^2}{\alpha^2}\frac{\partial^4\psi}{\partial\theta^2\partial\xi^2} + \frac{\beta^4}{\alpha^4}\frac{\partial^4\psi}{\partial\xi^4}$$

$$- i\frac{\epsilon^2}{\alpha^4}\frac{\partial^2\psi}{\partial\xi^2} = 0 \tag{3.6}$$

Let

$$\psi = f_n(\xi)\, e^{in\pi\theta} \tag{3.7}$$

Then (3.5) becomes

$$f_n^{iv} - \left(2\frac{\alpha^2n^2\pi^2}{\beta^2} + i\frac{\epsilon^2}{\beta^4}\right) f_n'' \frac{n^4\pi^4\alpha^4}{\beta^4} f_n = 0 \tag{3.8}$$

where primes denote differentiation with respect to ξ. Assuming solutions of (3.7) in the form

$$f_n = e^{\delta\xi} \tag{3.9}$$

we have from (3.8)

$$\delta^4 - 2\frac{\pi^2\alpha^2}{\beta^2}(n^2 + i\,\ell_o{}^2)\delta^2 + \frac{n^4\pi^4\alpha^4}{\beta^4} = 0 \tag{3.10}$$

where

$$\ell_o{}^2 = \frac{m\beta}{\pi\lambda} = \frac{2m\,R_o}{\lambda L_c} \tag{3.11}$$

At once, then

$$\delta^2 = \frac{\pi^2\alpha^2}{\beta^2}\left[(n^2 + i\,\ell_o{}^2) \pm \ell_o\,(-\ell_o{}^2 + 2i\,n^2)^{1/2}\right]$$

Now

$$(-\ell_o{}^2 + 2i\,n^2)^{1/2} = \frac{1}{\sqrt{2}}\left[(\bar{\ell}^2 - \ell_o{}^2)^{1/2} + i\,(\bar{\ell}^2 + \ell_o{}^2)^{1/2}\right]$$

$$\bar{\ell}^4 = \ell_o{}^4 + 4\,n^4$$

and hence

$$\delta^2 = \frac{\pi^2\alpha^2}{\beta^2}\left[\left\{n^2 \pm \frac{l_o}{\sqrt{2}}\,(\bar{l}^2 - l_o^2)^{1/2}\right\} + i\left\{l_o^2 \pm \frac{l_o}{\sqrt{2}}\,(\bar{l}^2 + l_o^2)^{1/2}\right\}\right]$$

(Note that plus sign goes with plus sign, minus with minus, from the previous equation.)

Let

$$r_1^2 = n^4 + l_o^4 + l_o^2\,\bar{l}^2 + \sqrt{2}\,l_o\left\{n^2\,(\bar{l}^2 - l_o^2)^{1/2} + l_o^2\,(\bar{l}^2 + l_o^2)^{1/2}\right\}$$

$$r_2^2 = n^4 + l_o^4 + l_o^2\,\bar{l}^2 - \sqrt{2}\,l_o\left\{n^2\,(\bar{l}^2 - l_o^2)^{1/2} + l_o^2\,(\bar{l}^2 + l_o^2)^{1/2}\right\}$$

then

$$\delta_1 = \pm\frac{\pi\alpha}{\beta\sqrt{2}}\left\{\left[r_1 + n^2 + \frac{l_o}{\sqrt{2}}\,(\bar{l}^2 - l_o^2)^{1/2}\right]^{1/2} + i\left[r_1 - n^2 - \frac{l_o}{\sqrt{2}}\,(\bar{l}^2 - l_o^2)^{1/2}\right]^{1/2}\right\}$$

$$= c_n + i\,d_n \qquad (3.12)$$

$$\delta_2 = \pm\frac{\pi\alpha}{\beta\sqrt{2}}\left\{\left[r_2 + n^2 - \frac{l_o}{\sqrt{2}}\,(\bar{l}^2 - l_o^2)^{1/2}\right]^{1/2} - i\left[r_2 - n^2 + \frac{l_o}{\sqrt{2}}\,(\bar{l}^2 - l_o^2)^{1/2}\right]^{1/2}\right\}$$

$$= (h_n + i\,k_n) \qquad (3.13)$$

Then

$$f_n(\xi) = \begin{cases} e^{\pm(c_n + i\,d_n)\xi} \\ e^{\pm(h_n + i\,k_n)\xi} \end{cases} \qquad (3.14)$$

and the homogeneous solution ψ may, therefore, be written from (3.7) as

$$\psi_H = \sum_{n=1}^{\infty} \left[A_n e^{(c_n+id_n)\xi} + B_n e^{-(c_n+id_n)\xi} + C_n e^{(h_n+ik_n)\xi} + D_n e^{-(h_n+ik_n)\xi} \right] e^{in\pi\theta} \tag{3.15}$$

C. LOADING ON THE ROUND SHANK AND A PARTICULAR SOLUTION OF EQUATION (3.4)

Consider the centrifugal loading defined by

$$\begin{aligned} P_\xi^{(A)} &= \rho_o \omega^2 h_A (\ell_T - z_A) && 0 \le z_A \le \ell_A \\ P_\xi^{(B)} &= \rho_o \omega^2 h_B (\ell_\epsilon + \ell_C + \ell_B - z_B) && 0 \le z_B \le \ell_B \\ P_\xi^{(C)} &= \rho_o \omega^2 h_C (\ell_\epsilon + \ell_C - z_C) && 0 \le z_C \le \ell_C \end{aligned} \tag{3.16}$$

where ω is the angular velocity and the superscripts identify the component of the propeller. We rewrite (3.16) in the form

$$\begin{aligned} P_\xi^{(A)}(\xi) &= \rho_o \omega^2 h_A \ell_A \left(\frac{\ell_T}{\ell_A} - \xi \right) \\ P_\xi^{(B)}(\xi) &= \rho_o \omega^2 h_A \ell_B (1 + \bar{b}\xi) \left(\frac{\ell_{\epsilon CB}}{\ell_B} - \xi \right) \\ P_\xi^{(C)}(\xi) &= \rho_o \omega^2 h_C \ell_C \left(\frac{\ell_{\epsilon C}}{\ell_c} - \xi \right) \end{aligned} \tag{3.17}$$

and note that as a consequence of this and using (2.9)

$$\begin{aligned} A_\xi^{(A)}(\xi) &= \frac{L_A}{\alpha} \int_o^\xi P_\xi^{(A)} \, d\xi \\ A_\xi^{(B)}(\xi) &= \frac{L_B}{\alpha} \int_o^\xi P_\xi^{(B)} \, d\xi + A_\xi^{(A)}(1) \\ A_\xi^{(C)}(\xi) &= \frac{L_C}{\alpha} \int_o^\xi P_\xi^{(C)} \, d\xi + A_\xi^{(B)}(1) \end{aligned} \tag{3.18}$$

In (3.17), we have assumed that h_A and h_C are constants while h_B varies linearly

$$h_B = h_A (1 + \bar{b}\xi)$$

$$\bar{b} = \frac{h_C}{h_A} - 1 \tag{3.19}$$

and we have defined (see Fig. 1)

$$\ell_{\epsilon C} = \ell_\epsilon + \ell_C$$

$$\ell_{\epsilon CB} = \ell_\epsilon + \ell_C + \ell_B = \ell_T - \ell_A \tag{3.20}$$

Integrating (3.18) after substitution of (3.17), we have

$$A_\xi^{(A)}(\xi) = \frac{L_A}{\alpha} \rho_o \omega^2 h_A \ell_A \left(\frac{\ell_T}{\ell_A} \xi - \frac{\xi^2}{2} \right)$$

$$A_\xi^{(B)}(\xi) = \frac{L_B}{\alpha} \rho_o \omega^2 h_A \ell_B \left[\frac{\ell_{\epsilon CB}}{\ell_B} \xi - \left(1 - \bar{b} \frac{\ell_{\epsilon CB}}{\ell_B} \right) \frac{\xi^2}{2} - \frac{\bar{b}}{3} \xi^3 \right] + A_\xi^{(A)}(1) \tag{3.21}$$

$$A_\xi^{(C)}(\xi) = \frac{L_C}{\alpha} \rho_o \omega^2 h_C \ell_C \left[\frac{\ell_{\epsilon C}}{\ell_C} \xi - \frac{\xi^2}{2} \right] + A_\xi^{(B)}(1)$$

Assuming

$$P_\theta = P = 0$$

then from (2.9), (2.13), and (2.14)

$$A_\theta = 0 \qquad \bar{q} = 0$$

$$q = \nu \frac{L_C}{\alpha} \alpha^2 \beta^2 \rho_o \omega^2 h_C \ell_C = q_o \tag{3.22}$$

$$\Omega = i \bar{K} q_o$$

and (3.4) may be written as

$$\alpha^4 \frac{\partial^4 \psi}{\partial \theta^4} + 2 \alpha^2 \beta^2 \frac{\partial^4 \psi}{\partial \theta^2 \, \xi^2} + \beta^4 \frac{\partial^4 \psi}{\partial \xi^4} - i \epsilon^2 \frac{\partial^2 \psi}{\partial \xi^2} = i \bar{K} q_o$$

A particular solution of this equation is

$$\psi_P = \frac{\bar{K}\, q_o}{2\,\epsilon^2}\,\xi^2$$

Substituting the expressions for $\bar{K}$, q_o, and ϵ^2, we have

$$\psi_P = -\frac{\nu}{2E}\left(\frac{\ell_C^2\, R_o}{L_C}\right)\rho_o\,\omega^2\,\xi^2 \tag{3.23}$$

We have finally

$$\psi = \psi_H + \psi_P \tag{3.24}$$

where ψ_H is given by (3.15), ψ_P by (3.23).

4. THE TRANSITION REGION B

A. INTRODUCTORY REMARKS

The transition region, as its name implies, refers to the transition from the airfoil section to the round shank of the propeller blade. Consequently, at one boundary of this region, the transverse section is circular while at the other boundary, the transverse section is elliptical. Considering the transition region as a shell, its middle surface is arbitrary, satisfying only the requirements that one edge is circular, the other elliptic. Because of the complexity of the equations governing the deformation of an arbitrary shell, some simplification is necessary. Rather than omit terms from these equations whose effect cannot be truly predicted, it is proposed to require that the middle surface of the transition region be developable. This means that the expressions for the Christoffel symbols of such a middle surface will be simplified so that on the surface the square of the line element may be expressed in the form $ds^2 = du^2 + dv^2$. As a consequence, the membrane equations of equilibrium can be solved in terms of a stress function and its first and second derivatives. To summarize, therefore, we must find

(i) A developable surface such that its boundary transverse sections are circular and elliptical.

(ii) Orthogonal geodesic coordinates u,v such that $ds^2 = du^2 + dv^2$.

B. CONSTRUCTION OF A DEVELOPABLE SURFACE

Let z be the axis connecting the centers of an ellipse and a circle which are parallel to each other, ℓ_B be the length from center to center along z

(see Fig. 1), and let the center of the ellipse be the origin of our coordinate system.

Consider a point P_o on the circle given by

$$P_o : (R_o \sin \phi_c , \quad R_o \cos \phi_c , \quad \ell_A + \ell_B) \tag{4.1}$$

and a point P_ϵ on the ellipse specified by

$$P_\epsilon : (a_1 \sin \phi_A , \quad b_1 \cos \phi_A , \quad \ell_A) \tag{4.2}$$

where R_o is the radius of the circle and a_1, b_1 are the semi-principal axes of the ellipse (see Fig. 1). By projecting the line $P_o P_\epsilon$ onto the x-z and y-z planes, it can be shown that the position vector $\vec{r} = \overrightarrow{P_\epsilon P_o}$ is given by

$$\vec{r} : \left[\frac{z^*}{\ell_B} R_o \sin \phi_c + \left(1 - \frac{z^*}{\ell_B}\right) \sin \phi_A ; \frac{z^*}{\ell_B} R_o \cos \phi_c + \left(1 - \frac{z^*}{\ell_B}\right) b_1 \cos \phi_A ; z^* + \ell_A \right]$$

or equivalently

$$\vec{r} : [\xi R_o \sin \phi_c + (1-\xi) a_1 \sin \phi_A ; \xi R_o \cos \phi_c + (1-\xi) b_1 \cos \phi_A ; \ell_B \xi + \ell_A] \tag{4.3}$$

where

$$z^* = z - \ell_A , \qquad \xi = z^*/\ell_B$$

Equation (4.3) defines a ruled surface whose Gaussian curvature K must vanish if the surface is required to be developable, i.e.,

$$K = \frac{L N - M^2}{H^2} = 0$$

$$LN - M^2 = 0 \tag{4.4}$$

where, in the notation of Ref. 7,

$$L = \vec{n} \cdot \vec{r}_{11} , \qquad M = \vec{n} \cdot \vec{r}_{12} , \qquad N = \vec{n} \cdot \vec{r}_{22}$$

$$\vec{n} = \frac{\vec{r}_1 \times \vec{r}_2}{H} , \qquad H = |\vec{r}_1 \times \vec{r}_2| \tag{4.5}$$

$$\vec{r}_\alpha = \frac{\partial \vec{r}}{\partial \xi_\alpha} , \qquad \vec{r}_{\alpha\beta} = \frac{\partial^2 \vec{r}}{\partial \xi_\alpha \partial \xi_\beta}$$

ξ_1, ξ_2 being the parametric curves. We next choose z and ϕ_A as the two independent variables, and note that since $\vec{r}_{11} = 0$, L vanishes and with the use of (4.5), our condition for developability (4.4) becomes

$$\vec{r}_{12} \cdot (\vec{r}_1 \times \vec{r}_2) = 0 \tag{4.6}$$

Evaluation of (4.6) using (4.3) yields

$$\frac{d\,\phi_C}{d\,\phi_A} [b_1 \sin \phi_A \cos \phi_C - a_1 \cos \phi_A \sin \phi_C] = 0$$

whence we have the developability condition

$$\tan \phi_A = \eta_1 \tan \phi_C \tag{4.7}$$

where

$$\eta_1 = \beta_1^{-1} = \frac{a_1}{b_1} \tag{4.8}$$

The required developable surface, after substitution of (4.7) into (4.3), is therefore given by

$$\begin{aligned} x &= \sin \phi_C \left[R_o \xi + (1-\xi)\, a_1 \eta_1 \left\{ \frac{1 + \tan^2 \phi_C}{1 + \eta_1^2 \tan^2 \phi_C} \right\}^{1/2} \right] \\ y &= \cos \phi_C \left[R_o \xi + (1-\xi)\, b_1 \left\{ \frac{1 + \tan^2 \phi_C}{1 + \eta_1^2 \tan^2 \phi_C} \right\}^{1/2} \right] \\ z &= \ell_B \xi + \ell_A \end{aligned} \tag{4.9}$$

C. THE ORTHOGONAL GEODESIC COORDINATE SYSTEM

In finding an orthogonal geodesic coordinate system, we adopt the procedure given in Ref. 8, pp. 136-145. Since any straight line on a surface is a geodesic, it follows that ϕ_C = constant represents a system of geodesics. To this end, we define

$$\begin{aligned} u_1 &= 1 - \xi\,; & v_1 &= \frac{\pi}{2} - \phi_C \\ R &= \frac{R_o}{b_1}\,; & b &= \frac{b_1}{L_B} \\ f &= \left\{ \frac{1 + \tan^2 v_1}{\eta_1^2 + \tan^2 v_1} \right\}^{1/2}\,; & \ell &= \left(\frac{\ell_B}{L_B} \right)^2 \end{aligned} \tag{4.10}$$

and therefore rewrite (4.9) as

$$\vec{r}_D : \left(\frac{x}{L_B}, \frac{y}{L_B}, \frac{z}{L_B}\right)$$

$$\begin{aligned}
\frac{x}{L_B} &= b \cos v_1 \, [R + u_1(-R + \eta_1^2 f)] \\
\frac{y}{L_B} &= b \sin v_1 \, [R + u_1 (-R + f)] \\
\frac{z}{L_B} &= - \ell 1/2 \, u_1 + \frac{\ell_B + \ell_A}{L_B}
\end{aligned} \tag{4.11}$$

Introducing a new coordinate u_2 and assuming $u_1 = u_1(u_2, v_1)$, we can write

$$ds^2 = E_2 \, du_2^2 + 2 F_2 \, du_2 \, dv_1 + G_2 \, dv_1^2 \tag{4.12}$$

where

$$E_2 = \frac{\partial \vec{r}_D}{\partial u_2} \cdot \frac{\partial \vec{r}_D}{\partial u_2} = \bar{A}_o \left(\frac{\partial u_1}{\partial u_2}\right)^2$$

$$F_2 = \frac{\partial \vec{r}_D}{\partial u_2} \cdot \frac{\partial \vec{r}_D}{\partial v_1} = \frac{\partial u_1}{\partial u_2} \left[\bar{C} + \bar{A}_o \frac{\partial u_1}{\partial v_1}\right] \tag{4.13}$$

$$G_2 = \frac{\partial \vec{r}_D}{\partial v_1} \cdot \frac{\partial \vec{r}_D}{\partial v_1} = \bar{A} \left(\frac{\partial u_1}{\partial v_1}\right)^2 + \bar{B} + 2 \bar{C} \left(\frac{\partial u_1}{\partial v_1}\right)$$

and

$$\begin{aligned}
\bar{A}_o(v_1) &= b^2 \, [R^2 + 1 - 2 R f^{-1} - \eta_1^2 (1-\eta_1^2) \cos^2 v_1 f^2(v_1) + \ell/b^2] \\
\bar{B}(v_1) &= b^2 \, [R + u_1 (-R + \eta_1^2 f^3)]^2 \\
\bar{C}(v_1) &= b^2 (1 - \eta_1^2) \cos v_1 \sin v_1 f \, [R + u_1 (-R + \eta_1^2 f^3)]
\end{aligned} \tag{4.14}$$

It must be pointed out that use has been made of the identity

$$f' = \frac{df}{dv_1} = -(1 - \eta_1^2) \sin v_1 \cos v_1 f^3(v_1)$$

Requiring u_2 and v_1 to be orthogonal, i.e., $F_2 = 0$, we have

$$\frac{\partial u_1}{\partial v_1} = -\frac{\bar{C}}{\bar{A}_0} \tag{4.15}$$

or equivalently, by using (4.14)

$$\frac{\partial u_1}{\partial v_1} + q_1 u_1 = q_2 \tag{4.16}$$

where

$$\begin{aligned} q_1(v_1) &= (1 - \eta_1^2) \cos v_1 \sin v_1 f (-R + \eta_1^2 f^3) \bar{A}_0^{-1} \\ q_2(v_1) &= -R (1 - \eta_1^2) \cos v_1 \sin v_1 f \bar{A}_0^{-1} \end{aligned} \tag{4.17}$$

Noting that

$$\int q_1 \, dv_1 = \frac{1}{2} \log \bar{A}_0$$

we can formally write the solution of (4.16) as

$$\begin{aligned} u_1 &= \frac{g(u_2)}{\bar{A}_0^{1/2}(v_1)} - G^*(v_1) \\ G^*(v_1) &= \frac{R(1-\eta_1^2)}{\bar{A}_0^{1/2}} \int \frac{\cos v_1 \sin v_1 f(v_1)}{\bar{A}_0^{1/2}} \, dv_1 \end{aligned} \tag{4.18}$$

With u_1 as defined by (4.18), (4.12) may now be written after substituting for E_2 as given by (4.13), as

$$ds^2 = \bar{A}_0 \left(\frac{\partial u_1}{\partial u_2}\right)^2 du_2^2 + G_2 \, dv_1^2 \tag{4.19}$$

We now set

$$u_3 = \int \bar{A}_0^{1/2} \frac{\partial u_1}{\partial u_2} \, du_2$$

so that (4.19) becomes

$$ds^2 = du_3^2 + G_2\, dv_1^2 \tag{4.19a}$$

From (4.18)

$$\frac{\partial u_1}{\partial u_2} = \frac{1}{\bar{A}_0^{1/2}} \frac{dg(u_2)}{du_2}$$

i.e.,

$$u_3 = \int \frac{dg}{du_2}\, du_2 = g(u_2)$$

and (4.18) becomes

$$u_1 = \frac{u_3}{\bar{A}_0^{1/2}} - G^*(v_1) \tag{4.20}$$

from which u_3 may be expressed in terms of u_1 and v_1. Applying the orthogonality condition (4.15) to the expression for G_2 in (4.13), we have

$$G_2 = \bar{B} - \frac{\bar{C}^2}{\bar{A}_0} = \bar{B}\left[1 - (1-\eta_1^2)^2 \cos^2 v_1 \sin^2 v_1 f^2(v_1)\bar{A}_0^{-1}\right]$$

Substituting for $\bar{B}$ from (4.14) and for u_1 from (4.20), we finally obtain

$$\sqrt{G_2} = C_1(v_1)\, u_3 + C_2(v_1) \tag{4.21}$$

where

$$C_1(v_1) = \left\{1 - \frac{(1-\eta_1^2)^2 \cos^2 v_1 \sin^2 v_1 f^2(v_1)}{\bar{A}_0(v_1)}\right\}^{1/2} \frac{[-R + \eta_1^2 f^3(v_1)]}{\bar{A}_0^{1/2}(v_1)} \tag{4.22}$$

$$C_2(v_1) = \left\{1 - \frac{(1-\eta_1^2)^2 \cos^2 v_1 \sin^2 v_1 f^2(v_1)}{\bar{A}_0(v_1)}\right\}^{1/2} R\left\{1 - \frac{G^*(v_1)}{R}[-R+\eta_1^2 f^3(v_1)]\right\}$$

If $C_2(v^*) = 0$, then if we let

$$v_2 = \int C_1(v_1)\, dv_1 \tag{4.23}$$

then (4.19a) becomes

$$ds^2 = du_3^2 + u_3^2 \, dv_2^2 \tag{4.24}$$

Finally, if we define

$$\begin{aligned} u &= u_3 \cos v_2 \\ v &= u_3 \sin v_2 \end{aligned} \tag{4.25}$$

Equation (4.24) reduces to the form

$$ds^2 = du^2 + dv^2 \tag{4.26}$$

APPENDIX

B. T. Caldwell

LOADING OF THE ELLIPTIC CYLINDER

In the ξ-direction, there is an effective loading component

$$P_\xi(\xi) = \rho_o \omega^2 \ell_A h_A \left(\frac{\ell_T}{\ell_A} - \xi\right) \tag{A1}$$

where ρ_o is the density of the material, ω is the angular velocity, and $\ell_T = \ell_A + \ell_B + \ell_C + \ell_\epsilon$ as shown in Fig. 1.

In the θ-direction, the loading component is negligible, i.e.,

$$P_\theta = 0$$

In the ζ-direction, we assume P to have the following form:

$$P(\xi_1\theta) = \bar{p}_o [1 - S(\theta)] p_1(\xi) \tag{A2}$$

where $\bar{p}_o$ is a constant, and

$$p_1(\xi) = \sum_{n=0}^{\infty} a_{2n+1} \sin (2n+1) \pi\xi \tag{A3}$$

In (A3), the coefficients a_m will be so chosen that $p_1(\xi)$ varies as an ellipse of major axis ℓ_A and of arbitrary minor axis. In order to find a representative form for $S(\theta)$ in (A2), we select a typical pressure distribution for the airflow around a thin airfoil. To this end, we make use of the data given on p. 328 of Ref. 2 for an airfoil which sufficiently approximates the elliptic section so that the general nature of the results will hold for our study. The formula used for the determination of S is taken from p. 77 (loc. cit.) as are the following quotations with our comments in parentheses:

"The velocity distribution about the wing-section is thus considered to be composed of three separate independent components as follows:

1. The distribution corresponding to the velocity distribution over the basic thickness form at zero angle of attack (v).
2. The distribution corresponding to the load distribution of the mean line at its ideal angle of attack (Δv; in this particular case $\Delta v = 0$ because the airfoil and the ellipse are both symmetric about the horizontal axis).

3. The distribution corresponding to the additional load distribution associated with the angle of attack (Δv_α).

"The local load at any chordwise position is caused by a difference of velocity between the upper and lower surfaces. It is assumed that the velocity increment on one surface is equal to the velocity decrement on the other surface." And from p. 79 comes the remark "although this method of superposition of velocities has inadequate theoretical justification, experience has shown that the results are adequate for engineering uses."

If V is the velocity at infinity, p_o the pressure at infinity, and ρ_a the mass density of air, then the pressure p_e at any point on the surface of a cylinder of infinite length is (cf. p. 77, Ref. 2)

$$p_e = H_p - \frac{1}{2} \rho_a V^2 S \tag{A4}$$

where

$$H_p = p_o + \frac{1}{2} \rho_A V^2 \tag{A5}$$

and

$$S = \left(\frac{v}{V} \pm \frac{\Delta v_\alpha}{V} \right)^2 \tag{A6}$$

the plus sign being used for the upper portion of the external boundary surface, the minus sign for the lower portion. S is readily found since v/V and $\Delta v_\alpha/V$ are tabulated on p. 328 of Ref. 2 for different values of percent of chord where the chord is the line of symmetry in this case (chord has the usual aeronautical definition). This means that the S computed for a given percent of chord is the value at the upper or lower intersection of the boundary surface with the perpendicular to the chord at the given percentage of chord length.

We now assume that the S of the airfoil at a given percent of chord is identical with the S of the elliptic middle surface at the same percent of chord. Knowing the percent of chord of the ellipse, we can find the length of arc corresponding to it.

In particular, we have

$$\bar{\theta} = \begin{cases} \frac{1}{S} (\bar{x}_A - \bar{x}_{AM}) , & \bar{x}_A \geq \bar{x}_{AM} \\ 1 - \frac{1}{S} (\bar{x}_{AM} - \bar{x}_A) , & \bar{x}_A \leq \bar{x}_{AM} \end{cases} \quad 0 \leq \bar{\theta} \leq 1 \tag{A7}$$

$$\bar{x}_A = \begin{cases} a_1[E(\theta',\pi/2)-E(\theta',\bar{\phi}], & 0 \le \frac{x_1}{100} \le 1/2, \ \pi \le \phi \le \frac{3\pi}{2} \\ a_1[E(\theta',\pi/2)+E(\theta',\bar{\phi}], & 1/2 \le \frac{x_1}{100} \le 1, \ \frac{\pi}{2} \le \phi \le \pi \\ a_1[3E(\theta',\pi/2)-E(\theta',\bar{\phi}], & 1 \ge \frac{x_1}{100} \ge 1/2, \ 0 \le \phi \le \frac{\pi}{2} \\ a_1[3E(\theta',\pi/2)+E(\theta',\bar{\phi}], & 1/2 \ge \frac{x_1}{100} \ge 0, \ \frac{3\pi}{2} \le \phi \le 2\pi \end{cases} \tag{A8}$$

$$0 \le \bar{x}_A \le g$$

$$E(\theta',\bar{\phi}) = \int_0^{\bar{\phi}} [1 - \sin^2 \theta' \sin^2 t]^{1/2} \, dt$$

$$s = 4 E(\theta',\pi/2)$$

$$\theta' = \arcsin (1 - \beta_1^2)^{1/2} \tag{A9}$$

$$\bar{\phi} = \arcsin \left| 2 \frac{x_1}{100} - 1 \right|$$

In the above equations, x_1 is the percent of chord, $\bar{x}_A$ is the arc length of the ellipse measured counterclockwise from the point $(-a_1,0)$, and $\bar{\theta}$ is a dimensionless coordinate whose origin occurs at $\bar{x}_{AM}$, the point of maximum pressure on the boundary surface. This point is determined from the condition [see Equation (A4)]:

$$\frac{v}{V} = \frac{\Delta v \alpha}{V} \tag{A10}$$

Evaluating the elliptic integrals $E(\theta',\bar{\phi})$ by means of Refs. 4 and 5 and using Equations (A7) to (A10), we compute $S(\bar{\theta}_j)$ at $\bar{\theta}_j$ which are discrete values of $\bar{\theta}$. This computation is given in Table I. The values of the constants used are

$$a_1 = 5.3, \qquad b_1 = 0.2$$

$$\theta' = 87.837382^\circ \tag{A11}$$

whence, from (A10) and p. 328 of Ref. 2

$$\frac{\bar{x}_{AM}}{s} = 0.012042 \tag{A12}$$

TABLE I

CALCULATIONS LEADING TO THE FUNCTION $S(\bar{\theta}_j)$ AND THE FINAL RESULTS FOR $S(\bar{\theta})$

x_1	x_2/a_1	$\bar{\phi}$	$E(\theta;\bar{\phi})$	$\bar{x}_A/a_1$	$\frac{\bar{x}_A}{s}$	$\bar{\theta}_j$	$\left(\frac{v}{\bar{v}}\right)^*$	$\left(\frac{\Delta v_\alpha}{\bar{v}}\right)^*$	$\frac{v}{\bar{v}} \pm \frac{\Delta v_\alpha}{\bar{v}}$	$S(\bar{\theta}_j)$	$S(\bar{\theta})$
0	-1	90°	1.00296504	0	0	.987958	0	5.471	-5.471	29.93	29.93
1.25	- .975	77.161432°	.97585945	.02710559	.006756	.994714	1.029	1.376	- .347	.120	25.45
2.3	- .954	72.554012°	.954654530	.04831051	.012042	0	1.040	1.040	0	0	0
2.5	- .95	71.805128°	.95062706	.05233798	.013046	.001004	1.042	.980	+ .062	.0038	.008
5.	- .9	64.158067°	.90040715	.10255789	.025564	.013522	1.047	.689	.358	.128	.109
7.5	- .85	58.211669°	.85028905	.15267599	.038056	.026014	1.051	.557	.494	.244	.207
10	- .8	53.130102°	.80021254	.20275250	.050538	.038496	1.053	.476	.577	.333	.301
15	- .7	44.427004°	.70011909	.30284595	.075488	.063446	1.055	.379	.676	.457	.470
20	- .6	36.869898°	.60006632	.40289872	.100427	.088385	1.057	.319	.738	.545	.614
30	- .4	23.578178°	.40001683	.60294821	.150291	.138249	1.060	.244	.816	.666	.747
40	- .2	11.536959°	.20000195	.80296309	.200147	.188105	1.064	.196	.868	.753	.751
50	0	0°	0	1.00296504	.25	.237958	1.066	.160	.906	.821	.705
60	.2	11.536959°	.20000195	1.20296699	.299853	.287811	1.068	.130	.938	.880	.712
70	.4	23.578178°	.40001683	1.40298187	.349709	.337667	1.064	.104	.960	.922	.822
80	.6	36.869898°	.60006632	1.60303136	.399573	.387531	1.051	.077	.974	.949	1.001
90	.8	53.130102°	.80021254	1.80317758	.449462	.437420	1.017	.049	.968	.937	1.160
95	.9	64.158067°	.90040715	1.90337219	.474436	.462394	.981	.032	.949	.901	1.204
100	1	90°	1.00296504	2.00593008	.5	.487958	0	0	0	0	1.217
95	.9	64.158067°	.90040715	2.10848795	.525564	.513522	.981	.032	1.013	1.026	1.198
90	.8	53.130102°	.80021254	2.20868256	.550538	.538496	1.017	.049	1.066	1.136	1.156
80	.6	36.869898°	.60006632	2.40882878	.600427	.588385	1.051	.077	1.128	1.272	1.071
70	.4	23.578178°	.40001683	2.60887827	.650291	.638249	1.064	.104	1.168	1.364	1.057
60	.2	11.536959°	.20000195	2.80889315	.700147	.688105	1.068	.130	1.198	1.435	1.241
50	0	0°	0	3.00889510	.75	.737958	1.066	.160	1.226	1.503	1.595
40	- .2	11.536959°	.20000195	3.20889705	.799853	.787811	1.064	.196	1.260	1.588	1.974
30	- .4	23.578178°	.40001683	3.40891193	.849709	.837667	1.060	.244	1.304	1.700	2.155
20	- .6	36.869898°	.60006632	3.60896142	.899573	.887531	1.057	.319	1.376	1.893	1.945
15	- .7	44.427004°	.70011909	3.70901419	.924512	.912470	1.055	.379	1.434	2.056	1.672
10	- .8	53.130102°	.80021254	3.80910764	.949462	.937420	1.053	.476	1.529	2.338	1.372
7.5	- .85	58.211669°	.85028905	3.85918415	.961944	.949902	1.051	.557	1.608	2.586	1.099
5.	- .9	64.158067°	.90040715	3.90930225	.974436	.962394	1.047	.689	1.736	3.014	2.508
2.5	- .95	71.805128°	.95062706	3.95952216	.986954	.974912	1.042	.980	2.022	4.088	.748
1.25	- .975	77.161432°	.97585945	3.98475455	.993244	.981202	1.029	1.376	2.405	5.784	5.792
0	-1.	90°	1.00296504	4.01186014	1.	.987958	0	471	5.471	29.93	29.93

*The data in this column are taken from the experimental data of Ref. 2, p. 328.

There remains the task of finding a simple functional relationship between $S(\bar{\theta}_j)$ and $\bar{\theta}$. We note from the results of our previous computation that S has a high peak occurring at

$$\bar{\theta}_{j_o} = 1 - \frac{\bar{x}_{AM}}{s} :$$

$$S(\bar{\theta}_{j_o}) = S_{j_o} = 29.665 \tag{A13}$$

We assume, therefore, that S has the form

$$S(\bar{\theta}) = \sum_{n=1}^{\infty} B_n \sin n\pi\bar{\theta} + F_1(\bar{\theta}) \tag{A14}$$

$$F_1(\bar{\theta}) = A_1 [\sin^2 2 m\pi\bar{\theta}] \left(\bar{\theta} + \frac{\bar{x}_{AM}}{s}\right)^{k_o} \tag{A15}$$

and impose the following conditions for the determination of $F_1(\bar{\theta})$:

(i) $F_1(\bar{\theta}_{j_o}) = A_1 \pm \delta \ , \ \delta > 0$

(ii) $F_1(\bar{\theta}_{j_o}) = S_{j_o}$

(iii) $F_1(\bar{\theta}_{j_o-1}) = S_{j_o-1} = 5.373$

Condition (i) implies that

$$\sin 2 m\pi \frac{\bar{x}_{AM}}{s} = \sin \frac{\pi}{2}$$

i.e.,

$$m = 21$$

$$\sin^2 2 m\pi \left(1 - \frac{\bar{x}_{AM}}{s}\right) = 0.9996 \tag{A16}$$

From (A16) and (ii)

$$A_1 \sin^2 2 m\pi \left(1 - \frac{\bar{x}_{AM}}{s}\right) = 29.665$$

i.e.,

$$A_1 = 29.68 \tag{A17}$$

From (A15) and (A17), and from the computed data noting that $\bar{\theta}_{j_o-1} = 0.981202$

$$(0.993244)^{k_o} = 0.4801$$

i.e.,

$$k_o = 108 \tag{A18}$$

where the nearest integral value of k_o is used.

The values of B_n are evaluated in the usual manner yielding

$$\begin{aligned} B_1 &= 1.451 & B_3 &= 0.5676 \\ B_2 &= -0.4966 & B_4 &= -0.3070 \\ & & B_5 &= 0.3280 \end{aligned} \tag{A19}$$

Five terms of the Fourier series are sufficient for satisfactory convergence. We have, therefore

$$S(\bar{\theta}) = \sum_{n=1}^{5} B_n \sin n\pi\bar{\theta} + 29.68\,[\sin^2 42\,\pi\bar{\theta}]\,(\bar{\theta} + 0.012042)^{108} \tag{A20}$$

The plot of $S(\bar{\theta})$ together with that of the function $S(\bar{\theta}_j)$ is shown in Fig. 2.

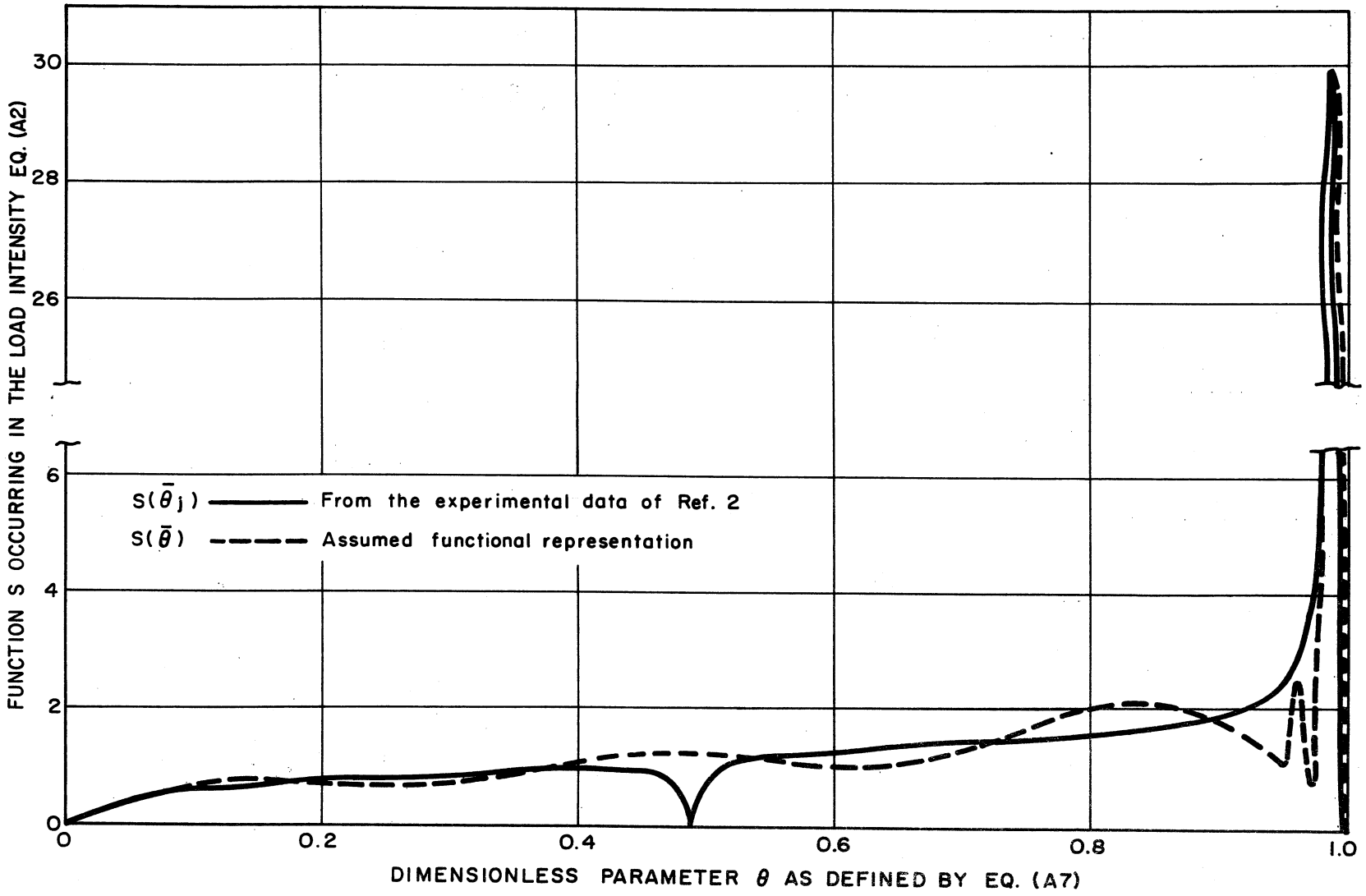
FUNCTION S OCCURRING IN THE LOAD INTENSITY EQ. (A2)
30
28
26
6
4
2
0
$S(\bar{\theta}_j)$ From the experimental data of Ref. 2
$S(\bar{\theta})$ Assumed functional representation
0
0.2
0.4
0.6
0.8
1.0
DIMENSIONLESS PARAMETER θ AS DEFINED BY EQ. (A7)

Fig. 2.

REFERENCES

1. A. E. Green and W. Zerna, Theoretical Elasticity, Oxford Univ. Press, New York, 1954.

2. Ira H. Abbott and Albert E. von Doenhoff, Theory of Wing Sections, McGraw-Hill Book Co., New York, 1949.

3. Mathematical Tables Project, Table of ArcSin X, Columbia Univ. Press, 1945.

4. Tables of the Complete and Incomplete Elliptic Integrals, Reissued from Legendre's Traite des Fonctions Elliptiques, Paris, 1825, with an Introduction by Karl Pearson, F.R.S., Cambridge Univ. Press, New York, 1934.

5. Mathematical Tables Project, Tables of Lagrangian Interpolation Coefficients, Columbia Univ. Press, 1944.

6. Edoardo Storchi, "Integrazione delle equazioni indefinite della statica dei veli tesi su una generica superficie," Atti della Accademia Nationale dei Limei, Rendiconti, Classe di Scienze fisiche, Mathematiche e naturali, Volume 8, 1950, p. 326.

7. C. E. Weatherburn, Differential Geometry of Three Dimensions, Cambridge Univ. Press, New York, 1927.

8. D. J. Struik, Lectures on Classical Differential Geometry, Addison-Wesley Press, Cambridge, 1950.

PART II

EXPERIMENTAL STUDY

by

S. K. Clark

PREFACE

Models of three geometries of thin propeller blades were cast of aluminum alloy 355 and used for an experimental stress analysis comparing the effect on stresses of various transition sections. The blades were identical in both the hub and outboard (airfoil) sections, and differed only in the transition regions. Strain measurement in the transition region of each blade was accomplished by the use of stress-coat and electrical resistance strain gauges.

Loading fixtures were constructed which permitted the application of pure tensile loads and of pure bending moment about either the flat-wise or chord-wise axis of the blade. Two blades were loaded in tension and one in bending about the flat-wise axis in order to demonstrate the feasibility of the loading fixtures and the strain-measuring techniques.

GENERAL STATEMENT OF BACKGROUND

Work on the experimental phase of this program began in April, 1956, and approximately five months were consumed in planning tests and in the design of propeller blades and loading fixtures. Serious difficulty was encountered in finding acceptable methods of manufacturing the blades, since machining proved to be too costly and since only one foundry was willing to attempt direct casting on the blades. In view of the limited financial resources of the project, it was decided to attempt casting, and a contract for this was let to Pressure Cast Products, Inc., 1028 Vermont Ave., Detroit 16, Michigan, in November, 1956, with delivery promised for February 1, 1957. Considerable difficulty was experienced by this vendor in obtaining any kind of a casting, and after several months of unsuccessful trials a casting consultant was engaged by the project to provide advice to the vendor. Following this, complete castings were obtained, the last of the series being delivered July 20, 1957.

The castings as received were not acceptable from the standpoint of dimensional tolerances and contour shape. They were, however, sound and free from obvious flaws, and in light of this and considering that the project was now seriously short of time for completion of any testing it was decided to accept the castings. These castings were then machined and assembled in the fittings, and trial tests were run on two blades in tension and on one blade in bending. All fittings operated satisfactorily, and the method of applying loads and moments appears to be a sound one.

OBJECTIVES OF TEST PROGRAM

The general objective of the test program was to provide experimental data which could be used as verification of certain calculations to be made in the second year of theoretical work on this problem. It was decided in conference with Prof. P. M. Naghdi, director of the theoretical group, that it would be desirable to calculate from theory and to measure experimentally the stresses produced in an actual aerodynamic loading and by actual centrifugal loads. The experiment was originally designed to include loads as shown in Fig. 3.

The result of the loads is that each cross section of the transition region is acted upon by the following forces:

(a) A constant tensile force due to the mrw^2 of all material outside of the transition region.
(b) A variable tensile force due to the body force mrw^2 acting throughout the transition region.
(c) A bending moment which is variable and which is due to the presence of the aerodynamic pressure distribution. This bending moment has

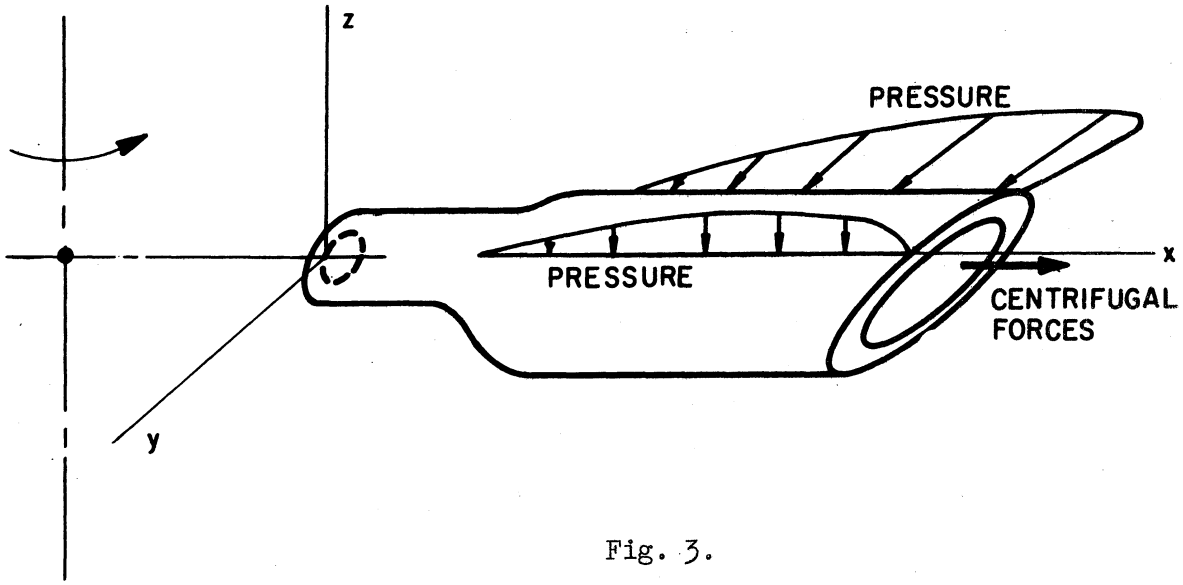

Fig. 3.

components in both the flat-wise and long-wise directions of the blade.

(d) A shear force due to the presence of the aerodynamic pressure distribution.

(e) A twisting moment or couple due to the possible eccentricity of the resultant of the aerodynamic forces.

It was decided to attempt to piece the complete loading together by performing a series of tests and by combining the results by superposition. In order to do this effectively, it was planned to request funds for a centrifugal test (covering loading "b" in the list above) and for an actual shear and bending loading test (items "c" and "d" above) during the anticipated second year of operation of the project. When it became evident that funds were not available for the second year of effort, it was decided to complete that part of the testing which would demonstrate the feasibility of the proposed loading schemes in so far as they had progressed. For this reason tensile and pure bending tests were chosen, since fittings were already manufactured for these tests and since the data obtained might be useful in propeller design. The methods of loading are explained in detail in the following sections.

METHODS OF LOADING

DIRECT TENSILE LOADS

Direct tensile loads were applied to the specimen by means of a conventional Riehle testing machine. Loading was accomplished through chain links as intermediate members, to insure that eccentricities did not introduce unwanted bending

moments. A blade loaded in this fashion is shown in Fig. 4. By means of these fittings loads of 40,000 total pounds could be easily applied in tension to the specimen.

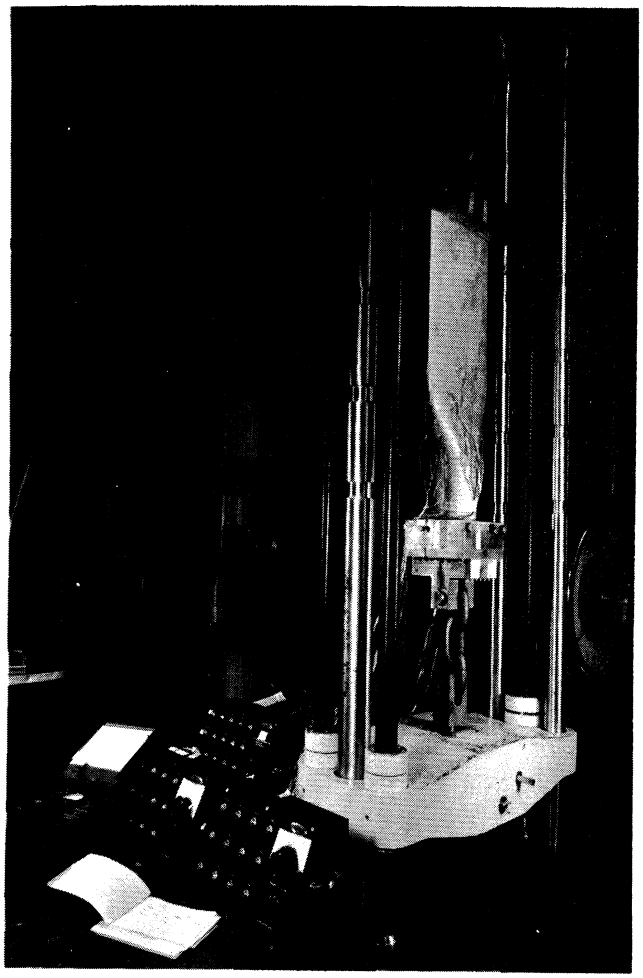

Fig. 4.

PURE BENDING MOMENT

A means for the application of pure bending moments without shear or tension was devised. In the form used here it is most easily described by the photograph of Fig. 5. Basically a single tensile load is split by means of cables and pulleys so that the specimen is subjected to 1/4 of this total load as each of four points as shown in Fig. 6.

The fittings for the blade models were constructed in such a way that this pure bending moment could be applied about either of the axes of the propeller blade.

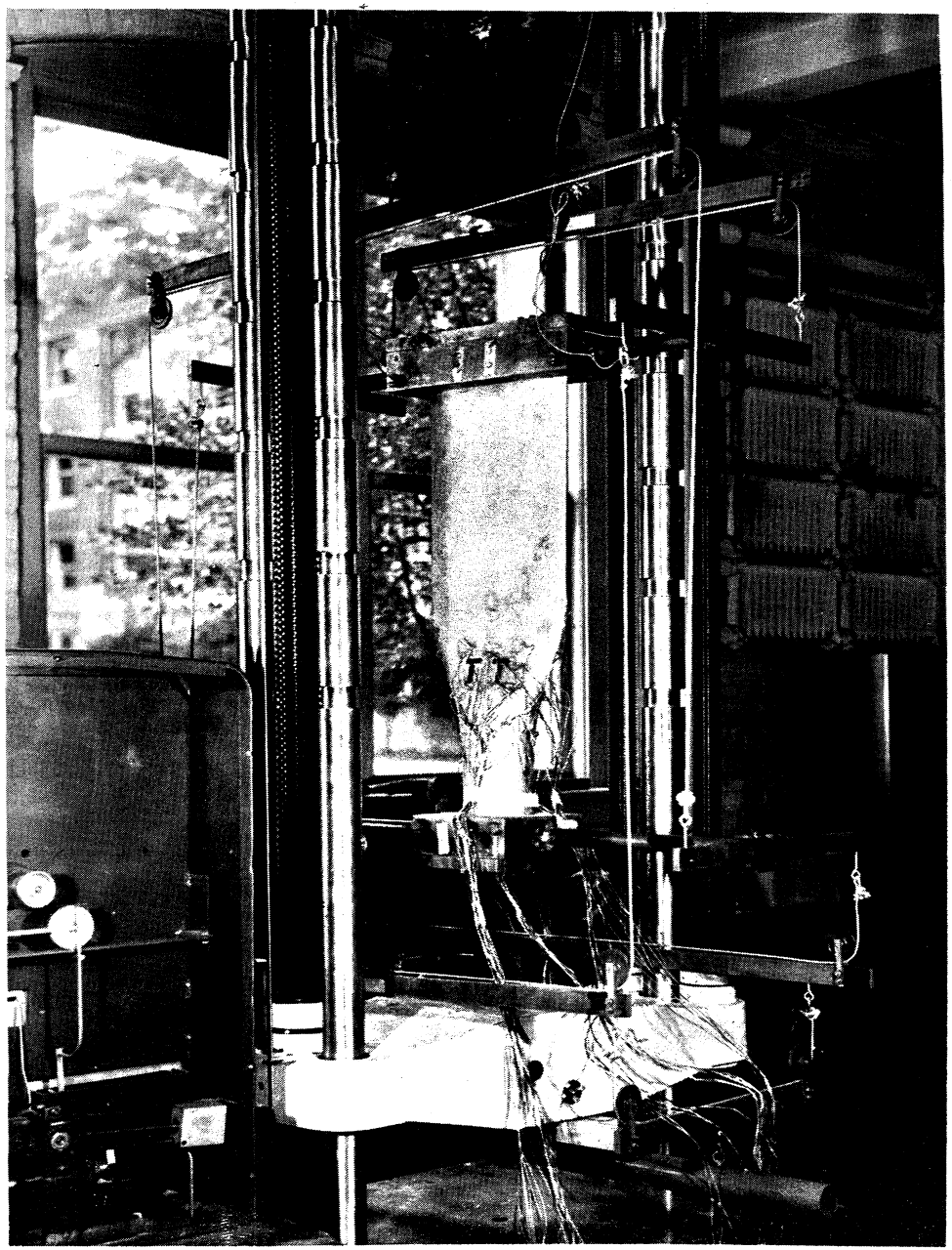

Fig. 5

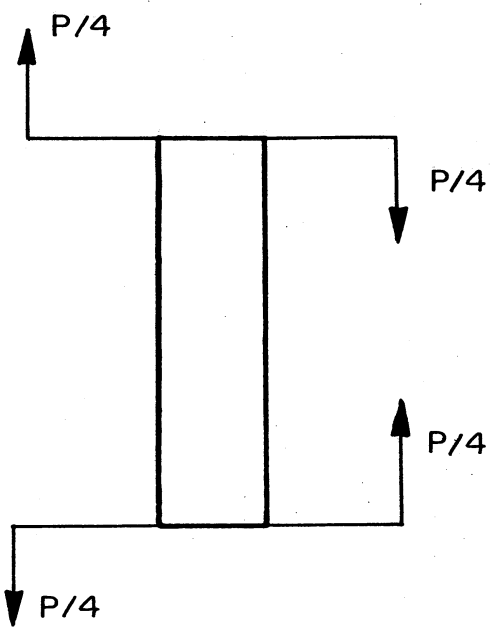

Fig. 6

INSTRUMENTATION

Instrumentation of the propeller-blade models was performed by qualitative use of stress-coat and by electrical resistance strain gauges. Stress-coat was utilized to determine the directions of principal strain so that gauges might be properly oriented. It was not found possible to photograph the stress-coat pattern with enough clarity to present in this report.

Type A-18 strain gauges were placed on all models, both inside and outside, at 0%, 25%, 50%, 75%, and 100% of the transition length, measured from the root end of the transition, and at other points as appeared desirable from the stress-coat tests. This particular type of gauge was chosen since its short length made installation in a restricted region somewhat easier, while the averaging effect of its length was kept small. At each of these sections along the transition length, a band of strain gauges was placed. These gauges were attached in pairs, one circumferential and one aligned with the longitudinal axis of the blade since the stress-coat tests indicated these to be the principal strain directions.

RESULTS

Due to the limited resources in time and funds it was not possible to perform as complete an interpretation of the measured strains as was desired. For this reason the results obtained are presented in summary form only, while the complete data are to be transmitted to WADC for possible further interpretation.

Tensile load strains were measured on the 12-inch and 6-inch transition-length models at loads of 10,000 and 20,000 pounds. The modulus of elasticity used in the calculations was determined by test to be 10×10^6 psi. Assuming that the gauge pairs are oriented in the principal strain directions, and assuming that the stress component through the thickness of the blade shell is zero, the stresses may be immediately computed in terms of the measured strains and the physical properties.

A very simple method of presenting these data is used, in which the ratio of maximum measured shear stress to nominal shear stress is tabulated. Nominal shear stress is defined as $1/2(P/A)$, where P = load and A = cross-sectional area. The maximum value of this ratio for each of the two transition sections tested is given in Table II.

TABLE II

Transition Section Length, in.	$(\tau_{meas}/\tau_{nom})_{max}$
6	2.35
12	1.62

For the bending test a couple of 2000-inch-pounds was applied about the flat axis of the 12-inch transition-length propeller blade and strains were again measured. Using the same assumptions as before, the maximum value of the measured bending strain may be converted to stress and divided by the nominal beam bending stress to yield a simple dimensionless ratio. Data of this nature from the 12-inch blade are given in Table III.

TABLE III

Transition Length, in.	$\left(\frac{\sigma_{b_{meas}}}{\sigma_{b_{nom}}}\right)_{max}$
12	1.89

Here, the nominal bending stress is taken to be Mc/I, and does not imply anything other than a convenient quantity for use in manufacturing a dimensionless ratio.

APPENDIX

BLADE GEOMETRY

The transition-section region was in all cases designed on the basis of one half cycle of a cosine curve. As an example, the two lines of Fig. 7 may be joined by a curve, shown as a dotted line, of the equation

$$y = \frac{b}{2}\left(1 - \cos\frac{\pi x}{\ell}\right)$$

which satisfies both ordinate and slope continuity. Curves of this type were fitted to each of the two plan views (side and front) of each of the three lengths of transition section, for both inside and outside profiles. The cross section of each blade, again both inside and outside, was taken to be an ellipse whose major and minor axes were chosen to conform with the half-cosine curve previously discussed. The constant outboard section was also defined by ellipses. Thus, the shell in all cases is defined as the material lying between two concentric ellipses, with the circular shank merely a special case of this. It should be pointed out that this definition of shape is almost identical with that which would be obtained in the usual manner of fairing with splines. Blade drawings are given in Plates I through IV.

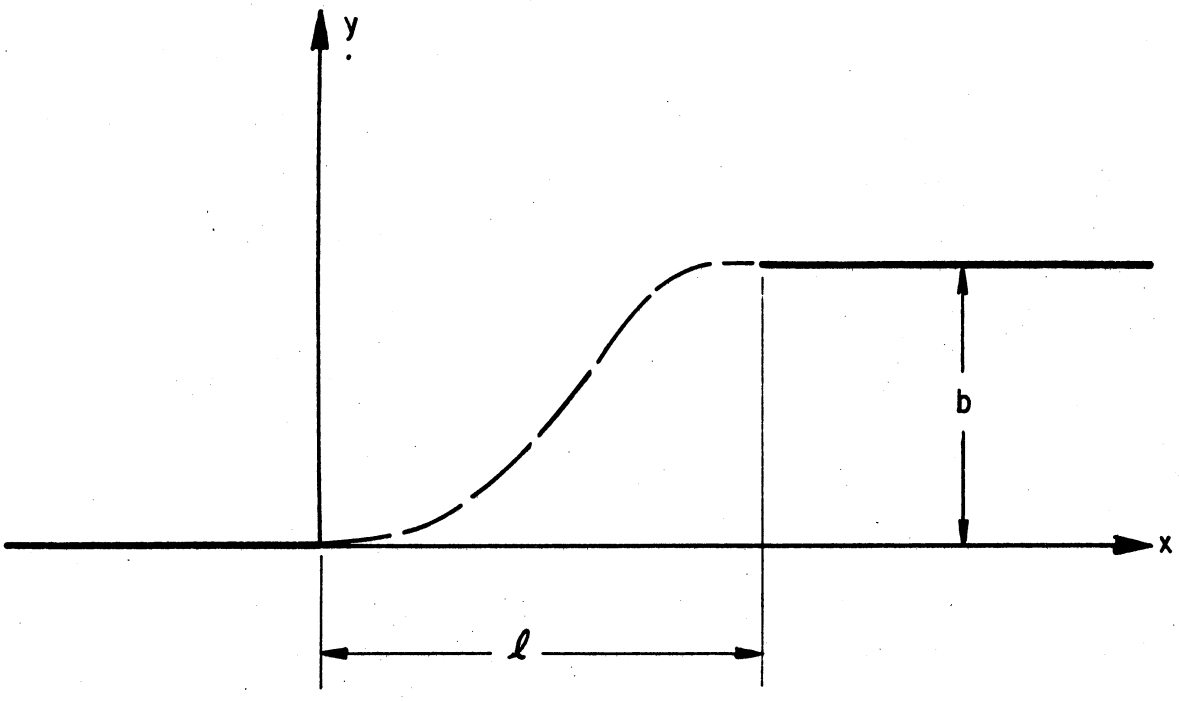

Fig. 7.